scientific reports

Check for updates

OPEN

Ultra-conformable tattoo electrodes for providing sensory feedback via transcutaneous electrical nerve stimulation

Mascia Antonello[1,3], Collu Riccardo[1,3]✉, Paolini Roberto[2], Demofonti Andrea[2], Cordella Francesca[2], Zollo Loredana[2]✉, Barbaro Massimo[1]✉ & Cosseddu Piero[1]✉

Electrical stimulation of the peripheral nervous system has been demonstrated to be effective in restoring somatotopic sensory information in subjects with amputations. It can be achieved using invasive electrodes, which require surgical implantation, or non-invasive electrodes, which are applied directly to the skin. Whereas less selective, non-invasive electrodes offer the advantage of avoiding surgical procedures. Additionally, commercially available wet Ag/AgCl electrodes lack adaptability to the irregular surface of a subject's residual limb, leading to detachment during movement or use. This study aims to address some of the limitations of non-invasive electrodes by proposing and validating the use of ultra-conformable Parylene C-based tattoo electrodes to restore somatotopic sensory information through transcutaneous electrical stimulation of the peripheral nervous system. The skin-electrode impedance was characterized in a healthy subject at varying frequencies over nine hours, showing a maximum impedance variation of 8% at the target stimulation frequency. Then, the performance of the proposed tattoo technology was compared to that of commercial Ag/AgCl electrodes through experimentation involving 12 healthy participants. The study found no statistically significant differences in key stimulation parameters (rheobase, $p > 0.3$, and chronaxie, $p > 0.15$) or in the sensory perceptions elicited by the two compared electrodes. Additionally, tattoo electrodes exhibited a lower operational impedance compared to commercial electrodes, highlighting their potential advantages for practical applications.

Keywords Electrical stimulation, Somatosensory sensations, Tattoo electrodes

Recent developments in the field of neuroprosthetics have shown how the integration of technologies for restoring the somatosensory information can provide benefits in prosthetic control[1–6], embodiment[7,8], prosthetic acceptance[9] and reduce abandonment[10], as well as a reduction in Phantom Limb Pain (PLP)[7,11,12]. While various methods for restoring tactile feedback through vibrotactile or mechanotactile[13,14] stimulations have been explored in the literature, and the electrical approach is the most promising. Indeed, it allows the elicitation of somatotopic and homologous sensations directly perceived in the patient's missing limb. [15–17]. The principle behind somatotopic electrical stimulation is to inject a specific charge into the sensory nerve fibers to recruit the neural portions that encode the sensations referred to the phantom limb. The effectiveness of the electrical stimulation has been demonstrated by using both invasive and non-invasive interfaces.

Particularly, invasive electrodes are divided into extraneural, such as cuff electrodes[18,19] and Flat Interface Nerve Electrodes (FINE), and intraneural, such as Longitudinal Intrafascicular Electrodes (LIFE[20],) Transversal Intraneural Multichannel Electrodes (TIME[21–23] and Utah Slanted Electrode Arrays (USEA[24].) The selectivity of a neural interface is often influenced by its level of invasiveness[25]. Although electrodes such as cuff and FINE have proven to be stable over the years[26,27], they are less selective than electrodes such as USEA and TIME, in which the active stimulation sites are in direct contact with the nerve fascicles, thus allowing the recruitment of more precise neural portions[24,28,29].

[1]Department of Electrical and Electronic Engineering, University of Cagliari, Cagliari, Italy. [2]Research Unit of Advanced Robotics and Human-Centered Technologies (CREO Lab), Università Campus Bio-Medico di Roma, Rome 00128, Italy. [3]Mascia Antonello and Collu Riccardo contributed equally to this work. ✉email: riccardo.collu@unica.it; l.Zollo@unicampus.it; massimo.barbaro@unica.it; piero.cosseddu@unica.it

Moreover, even if less selective than their implantable counterparts, noninvasive electrodes combined with Transcutaneous Electrical Nerve Stimulation (TENS) demonstrated good performance in restoring tactile feedback[30–41].

Different sensations can be elicited by modulating the stimulation parameters, such as frequency, amplitude, and shape of the stimulus[32,36,37,42]. Therefore, the electrode interface should guarantee the transmission of the different parameters over time without affecting the stimulation waveform.

A consensus on the kind of technology for the interface (i.e., electrode) between the stimulator and the skin is still lacking. While Ag/AgCl electrodes are the most commonly used interface for connecting stimulation devices to the skin due to their low skin-electrode impedance and ease of application, they have significant drawbacks. Their reliance on an electrolytic gel limits their suitability for long-term applications, as the gel degrades over time, leading to an increase in skin-electrode impedance and potential skin irritation[43,44]. Additionally, despite being commercially available in various shapes and sizes (e.g., round[45–48] or rectangular[39,49], these electrodes exhibit limited conformability to non-planar surfaces like an amputee stump, resulting in instability and discomfort during prolonged use[50]. To address these challenges, ultra-conformable tattoo electrodes offer a promising solution by adhering more securely and comfortably to the skin, thereby minimizing discomfort and irritation derived from traditional wet electrodes[51].

In the field of biological potential recording, where long-term measurements are crucial, dry electrodes have been developed to address the limitations mentioned above, eliminating the need for electrolyte gel or adhesive layers[52–54]. Although these electrodes typically exhibit higher electrode-skin impedance due to an increased capacitive component[55–58], they effectively prevent irritation while offering superior deformability and adhesion to the skin[59,60] also during prolonged use.

Among the various types of dry electrodes described in the literature, epidermal tattoo electrodes represent a promising option for transcutaneous somatotopic feedback applications. These electrodes adhere to the skin solely through weak electrostatic forces (i.e., van der Waals interactions), ensuring stable adhesion over time without the need for external support[61]. Thanks to this approach, ultra-thin, temporary, tattoo-based electrodes are capable of withstanding extreme mechanical deformation at small radii without compromising their functionalities. Moreover, such an approach ensures maximizing the contact area between the subject's skin and the tattoo electrode, a crucial feature for this kind of application since it enables reducing the contact impedance.

In addition, the employment of bio-compatible or chemically inert materials, such as Parylene C, allows for the minimization of adverse skin effects[51]. Thanks to these features, there is a plethora of examples of epidermal tattoo electrodes for bio-potential acquisition[51,62–65]. However, their application in sensory electrical stimulation systems has not been thoroughly investigated. In Table 1, the main related works in which epidermal electronics have been employed in augmented feedback or sensory feedback are presented. Although promising due to their non-invasiveness, vibrotactile or electro-tactile approaches lack a somatosensory match: the elicited sensation is perceived just locally on the stump and not in the missing limb[17,66,67]. Their working principle is based on sensory substitution, necessitating user training to recognize the artificial input. Nevertheless, the naturalness

Study	Material/Device	Thickness	Impedance (@500Hz)	Reusability	Stimulation	Application
Yuxiang Shi, et al.[68]	TENG-Polytetrafluoroethylene and Kapton (ion-bombarded for enhanced performance), PET, tin ball-shaped electrodes	//	//	yes	Current stimulation: 0–25 μA	virtual tactile displays, Braille instruction, intelligent protective suits, and nerve stimulation
Kuanming Yao, et al. [69]	Wireless electro-tactile system (WeTac). PDMS substrate, gold conductive traces, hydrogel electrodes (LiCl-based), flexible printed circuit board	170 μm			Current stimulation: 0–13.5 mA	Tactile feedback, virtual reality, and hand prosthetics
Weikang Lin, et al.[70]	5 × 5 fingertip electrode array is a piece of thin FPC with 25 copper pads; flexible printed circuit, rubber finger cot	//	//	yes	Voltage stimulation: 13–28 V	braille display, virtual reality shopping, and digital virtual experiences.
Baoxing Xu, et al. [71]	Multifunctional platform with electrotactile stimulation, electromyography, temperature, and strain sensing.	silicone elastomer 60 μm	//	no	Current stimulation: 3 mA	sensorimotor prosthetic control, management of lower back exertion, and electrical muscle activation.
Ming Ying, et al.[72]	ultrathin, stretchable silicon-based electronics and sensors mounted on the surfaces of elastomeric closed-tube structures for integration directly on the fingertips	Closed-tube structure 500 μm thick; electrotactile stimulating electrodes 1.2 μm	//	//	Stimulation through a diode: stable at 20 V, corresponding to currents of 0.25 mA	Human-machine interfaces, tactile sensing, and surgical gloves
Yahya Abbass, et al. [73]	screen-printed flexible sensor arrays based on P(VDF-TrFE) poly(vinylidene fluoride trifluoroethylene) piezoelectric polymer sensors, screen-printed on a transparent and flexible plastic foil substrate. A ferroelectric polymer P(VDF-TrFE) layer is then screen-printed onto the bottom electrodes, followed by screen printing of the top electrodes	175 μm thick flexible foil; PVDF 5.1 μm thick layer	//	//	Current stimulation: biphasic pulses in the range of 0–10 mA	Prosthetic application: mimicking spatially distributed natural feedback.
This work	Ultra-conformable and Ultrathin parylene-C-based gold electrodes	600 nm	< 5 kΩ	yes	Current stimulation: biphasic pulses in the range of 0.05 mA – 15 mA	Somatosensory Feedback, Transcutaneous Electrical Nerve Stimulation (TENS)

Table 1. Comparison of epidermal electronics for augmented feedback and sensory feedback.

and intuitiveness of sensory location and sensation are fundamental to improving dexterity and cognitive load during prosthetic wearing[17].

In this work, we propose for the first time the use of ultra-thin Parylene C-based tattoo electrodes for transcutaneous electrical stimulation of the median nerve to induce somatotopic sensations referred to the hand. We fabricated a 600 nm thick electrode, which, based on prior findings that films below 1 μm exhibit strong conformability to complex 3D surfaces without additional adhesive layers[74,75], is inherently conformal to ultrasoft substrates such as human skin via sole Van der Waals forces, as the bending stiffness EI, i.e., the ability of a structure to withstand bending or flexure under a load, exhibits a cubic dependence on the film thickness. We investigated the use of tattoo electrodes for sensory feedback on 12 full-able body subjects. We compared the behavior of tattoo electrodes with that of Ag/AgCl electrodes, examining the impact on both the physiological parameters of rheobase and chronaxie and on the quality and location of the sensations induced in the hand.

Results

Ultra-conformable tattoo electrode fabrication process

To optimize the electrical performance of the electrodes employed in non-invasive neurostimulation, it is fundamental to improve the electrode-skin interface to maximize the contact area between them. To achieve this, the tattoo electrodes developed in this work have been designed to maintain a total thickness below one micrometer, allowing the electrodes to adapt to the natural roughness of the skin. The fabrication process of the proposed ultra-comfortable tattoo electrodes is illustrated in Fig. 1.a. The whole procedure starts with a 125 μm-thick Poly(Ethylene Naphthalate) (PEN) substrate (i), onto which a water-soluble Poly(Vinyl Alcohol) (PVA) sacrificial layer is deposited throughout a standard spin coating technique and then backed at 90°C on a hot plate for 10 minutes (ii). This layer guarantees that all subsequent fabrication steps are completed without the premature detachment of the Parylene C nanofilm; it also helps prevent damage to the tattoo patch during the peel-off process. Next, the core of the tattoo electrode is created; a 500 nm-thick Parylene C layer is deposited via Chemical Vapor Deposition (CVD), and then gold electrodes, 50–70 nm thick, are deposited on top using thermal evaporation through a shadow mask (iv). The active area of the electrode has a diameter of about 25 mm. The electrode is peeled off from the plastic carrier to be applied to the skin and transferred to a piece of paper using a small amount of deionized water, which ensures the dissolution of the residual PVA layer (v). Once the water evaporates, the electrode can be stored or applied by wetting the back of the paper with a few drops of deionized water and gently sliding the paper off. The tattoo electrode is applied directly to the skin and is connected through an interconnection system made using a 13 μm-thick polyimide (KAPTON) substrate. Its reduced thickness enables the electrode to adhere to the skin conformably, maximizing the contact area, as shown in Fig. 1b. This feature allows the electrode to be used on irregular surfaces, such as the elbow, unlike commercial electrodes that often fail to maintain proper adhesion, as depicted in Fig. 1c. As can be seen in Fig. 1.d, it is worth mentioning that the resulting electrodes have a total thickness of less than 600 nm where the parylene occupies around 500nm and the gold layer is around 50nm. This ensures excellent conformal contact with the skin solely through electrostatic interactions, eliminating the need for glue or electrolyte gel. As demonstrated by Nawrocki et al.[76,77] ultra-thin films adhere to complex surfaces, such as human skin, through Van der Waals interactions, as the Bending Stiffness (EI) is proportional to the cube of the film thickness. Therefore, the proposed electrode thickness of less than 600 nm ensures an optimal electrode-skin adhesion."

Electrode storage capacitance was investigated according to Ganji et al.[78] through Cyclic Voltammetry analysis. Storage capacitance was estimated to be 1.46 mC/cm^2.

Electrode-skin contact impedance evaluation

To optimize the electrode dimensions for the proposed TENS applications, three sets of electrodes with varying areas were fabricated and tested in the frequency range from 20 to 500 Hz. The results were compared to the impedance measured using a set of five commercial pre-gelled electrodes in parallel[51,64,65,79]. Figure 1e reports the results for a set of 10 electrodes for each dimension (namely 1, 2, and 2.5 cm of diameter) applied on the same day (with one hour of the experiment) on the same subject, intending to reduce the inter-subject contact impedance variability. The best performance was obtained using electrodes with a diameter of 2.5 cm with an impedance of 27 ± 4 kΩ at 20 Hz and 4.15 ± 0.3 kΩ at 500 Hz. Impedance is a key characteristic in electrical stimulation since the higher the impedance, the higher the stimulator voltage compliance required to stimulate nerves and deliver the desired current effectively. Moreover, maintaining stable behaviors over time is a crucial characteristic of wearable applications. In this regard, the impedance of the tattoo electrode was measured over nine hours to observe the impedance variation over time. The higher impedance variation was recorded during the first hour of the test at 20 Hz, where it reached 15% of variaion with respect to the impedance measured at the beginning. As shown in Fig. 1f, the impedance at 500 Hz reached a maximum variation of approximately 8%. In addition, Supplementary Figure S1 reports the effect of the two electrodes on the subject's skin right after nine hours of measurements. It is possible to notice that Ag/AgCl electrodes cause redness and irritation of the skin due to the adhesive layer employed. In contrast, tattoo electrodes do not have any effect, as the adhesion with the skin is ensured solely by electrostatic interactions.

Strength duration curve – rheobase and chronaxie

We compared the stimulation performance of two categories of electrodes based on rheobase current and chronaxie time, two physiological parameters used to describe the excitability of a tissue[80], and that can be influenced by the kind of electrical stimuli that are applied[37,81–84]. Sensory and motor thresholds were collected for the electrodes at four different pulse width values: 300 μs, 400 μs, 500 μs, and 600 μs, respectively, according to stimulation ranges similar to those of previous studies[37,85]. Although median stimulation current values for

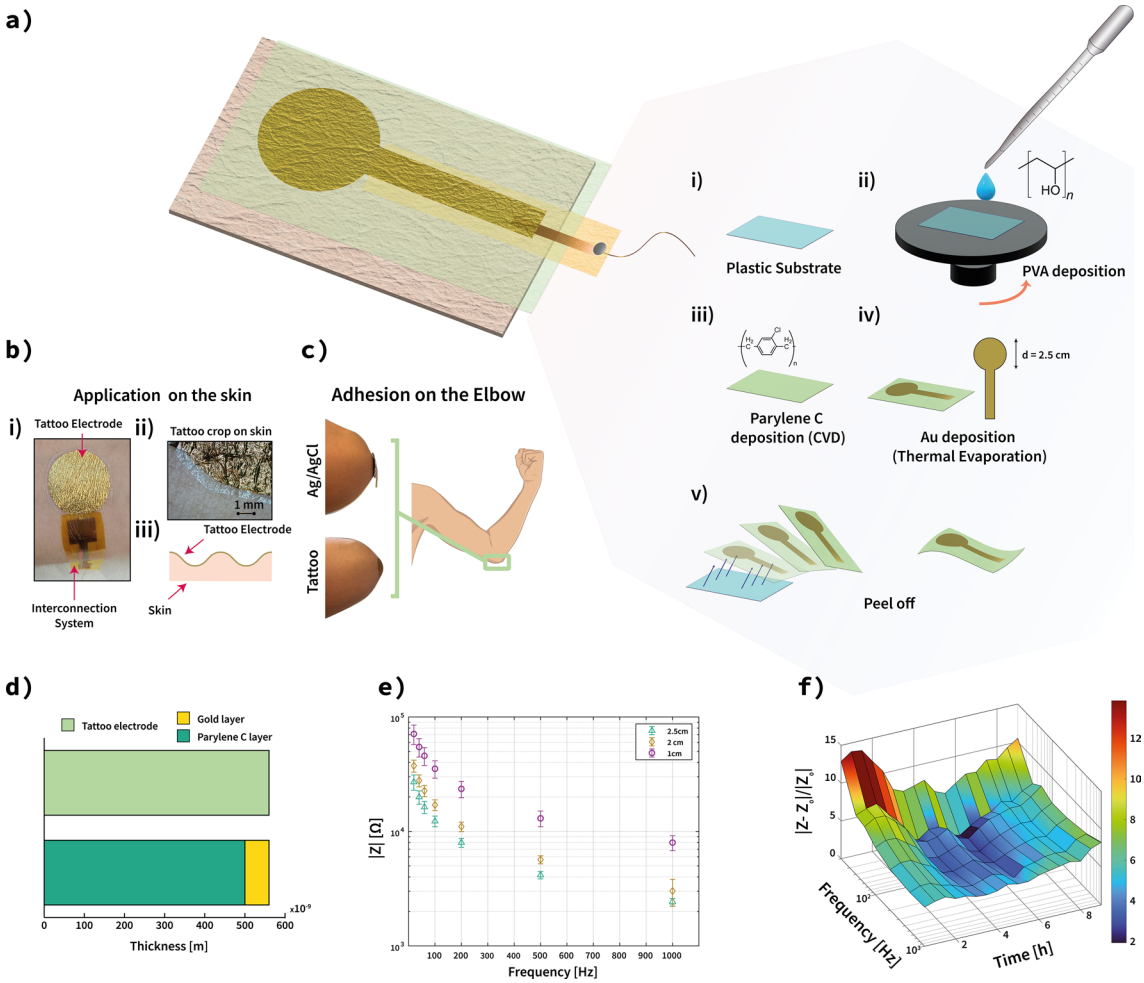

Fig. 1. Fabrication process and characterization of ultra-conformable Parylene C-based tattoo electrodes: A plastic substrate (a.i) served as the carrier throughout the fabrication process. Initially, a polyvinyl alcohol (PVA) sacrificial layer was deposited onto the substrate using a spin-coating technique (a.ii). a Parylene C layer was deposited via Chemical Vapor Deposition (a.iii), and a gold electrode (a.iv) was thermally evaporated on top of it. Subsequently, the tattoo electrode was peeled off from the carrier, thus obtaining the ultra-thin tattooable electrode (a.v). In this manner, the tattoo's active area remains at the bottom, while the top is covered and insulated by the parylene-C. The tattoo is applied to the skin, lying over an interconnection pad printed on Kapton (b.i). The tattoo follows the skin corrugation (b.ii), improving the total contact area between the tattoo and skin[74,75] (b.iii). The tattoo technology can adhere to irregular surfaces, such as the elbow, and remains securely attached. In contrast, the commercial Ag/AgCl technology does not ensure proper adhesion (c). The final dimension of the tattoo is less than 600 nm, where the parylene occupies around 500 nm and the gold layer is around 50 nm (d). Tattoo impedance was investigated at three different electrode dimensions (e). The impedance of one electrode with a diameter of 2.5 cm was monitored over nine hours of measurements, showing a maximum impedance variation of 15% at low frequency (20 Hz) and 8% at 500 Hz (f).

the tattoo electrodes are generally higher than commercial electrode ones, no statistical differences were found for sensory (Fig. 2a) and motor (Fig. 2b) thresholds. The sensory and motor threshold data were used to estimate the rheobase current and chronaxie time by fitting the Lapicque Eqs. [83,86,87], which describes the strength-duration curve, a relation between the minimum current required for stimulation and the pulse duration[87,88]. The Lapicque curve was fitted for each subject. Results from Lapicque fitting are consistent with the threshold analysis, as no statistically significant differences (Wilcoxon-ranksum) were observed between the rheobase current for sensory fibers ($p > 0.3$) and motor fibers ($p > 0.96$), as shown in Fig. 2c. In addition, there is no significant variation in chronaxie time ($p > 0.151$), as shown in Fig. 2d. The effective somatosensory stimulation area was investigated. We defined the effective stimulation area as the area comprised between the Lapicque curve for sensory fibers and the Lapicque curve for motor fibers, as represented in Fig. 2f. The sensory curve represents the lower limit for somatosensory feedback, as no sensations can be statistically elicited below it. At the same time, the motor curve represents the upper limit since, above it, slight movements of the digits of able-body volunteers will also accompany somatotopic sensations. We computed the effective somatotopic stimulation area for each subject for each pair of electrodes. The estimated effective somatotopic stimulation area

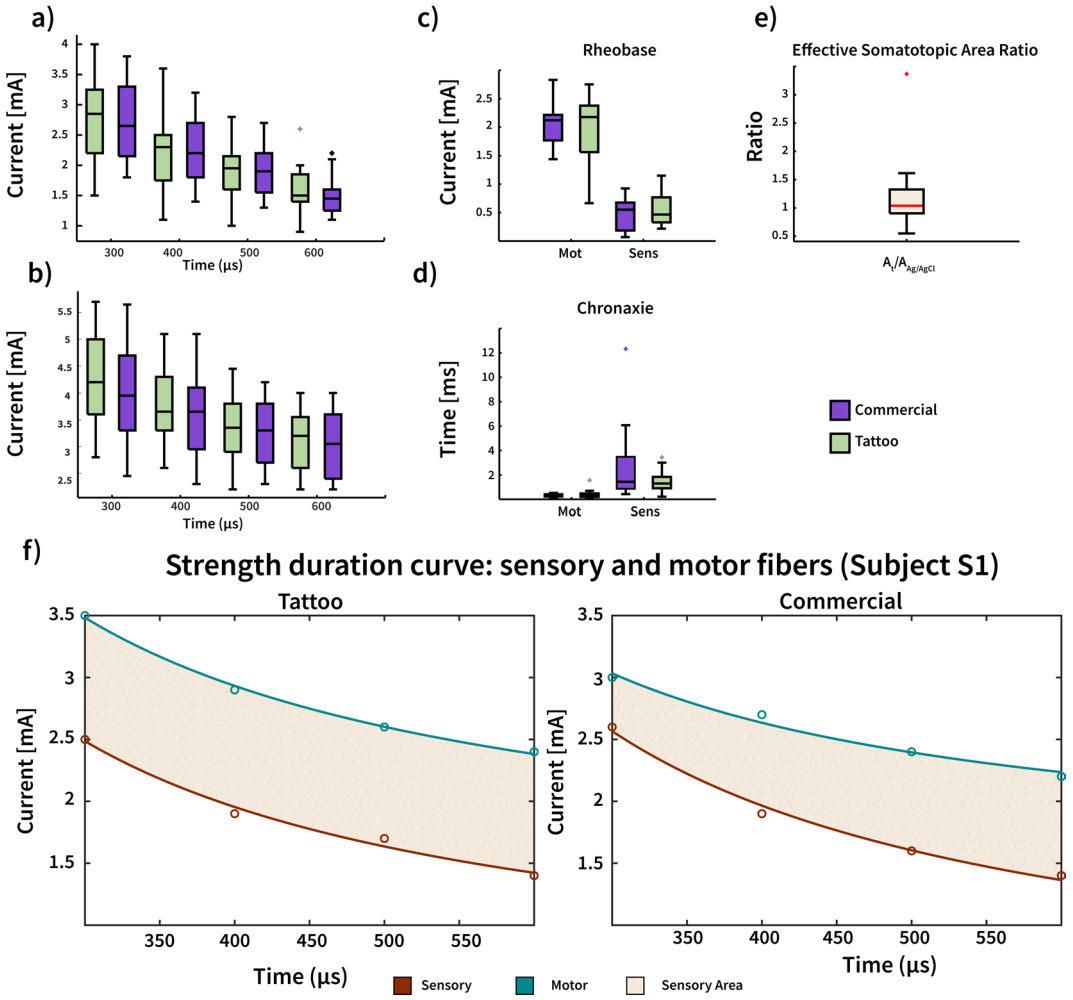

Fig. 2. Effect of electrodes on the strength-duration curve. The sensory threshold was investigated at four different pulse widths for both pairs of electrodes. No statistical differences were found between the electrodes (**a**).The motor threshold was investigated at four different pulse widths for both pairs of electrodes. No statistical differences were found between the electrodes (**b**). The thresholds were used to fit the Lapicque curve for sensory and motor fibers, obtaining rheobase and chronaxie for each subject. No statistical differences were obtained between the rheobase (**c**) and chronaxie (**d**) values. The area between the sensory and motor curves was computed for each subject for both electrodes, showing that the technology does not affect the effective somatotopic stimulation area for each subject ($p = 0.3804$) (**e**). The representation of the somatotopic sensation area for the tattoo and commercial electrodes for subject S1 (**f**). The red dots and curve illustrate the Lapicque curve for sensory feedback, which indicates the stimulation threshold for inducing somatotopic sensations referred to the hand. Similarly, the green dots and curve show the Lapicque curve for motor fiber activation. The area between the two curves defines the somatotopic sensory zone, representing the region where nerves can be stimulated without causing any visible activation of motor fibers.

of tattoo electrodes was then divided by the effective somatotopic stimulation area of the commercial electrodes, as shown in Fig. 2e. No significant variation was observed between the two areas ($p = 0.3804$).

Elicitation of somatotopic sensations

Somatosensations were collected by modulating the amplitude from the sensory threshold to the motor threshold, as shown in Fig. 3a-c-e. Tattoo electrodes elicited a higher number of sensations defined as "natural" (13.8% vs. 11.1%) and as "almost natural" (27.77% vs. 22.22%) with respect to Ag/AgCl technology. Even if the number of sensations reported as "superficial" is comparable between the two electrodes (52.77% vs. 55,55%), tattoo technology reported a higher number of sensations reported as "deep" (44.44% vs. 30,55%). The global hand coverage of the two technologies is comparable between the electrodes, even if the Ag/AgCl technology reported generally better coverage of fingers.

Afterward, we modulated the stimulation frequency between 100 Hz and 500 Hz, collecting Somatosensations, as shown in Fig. 3b-d-f. Tattoo electrodes elicited a higher number of sensations defined as "natural" (10% vs. 8,33%) and as "almost natural" (15% vs. 10%) with respect to Ag/AgCl technology. Although Tattoo electrodes elicited mainly sensations located superficially on the skin (53,33%), they also elicited a higher number of

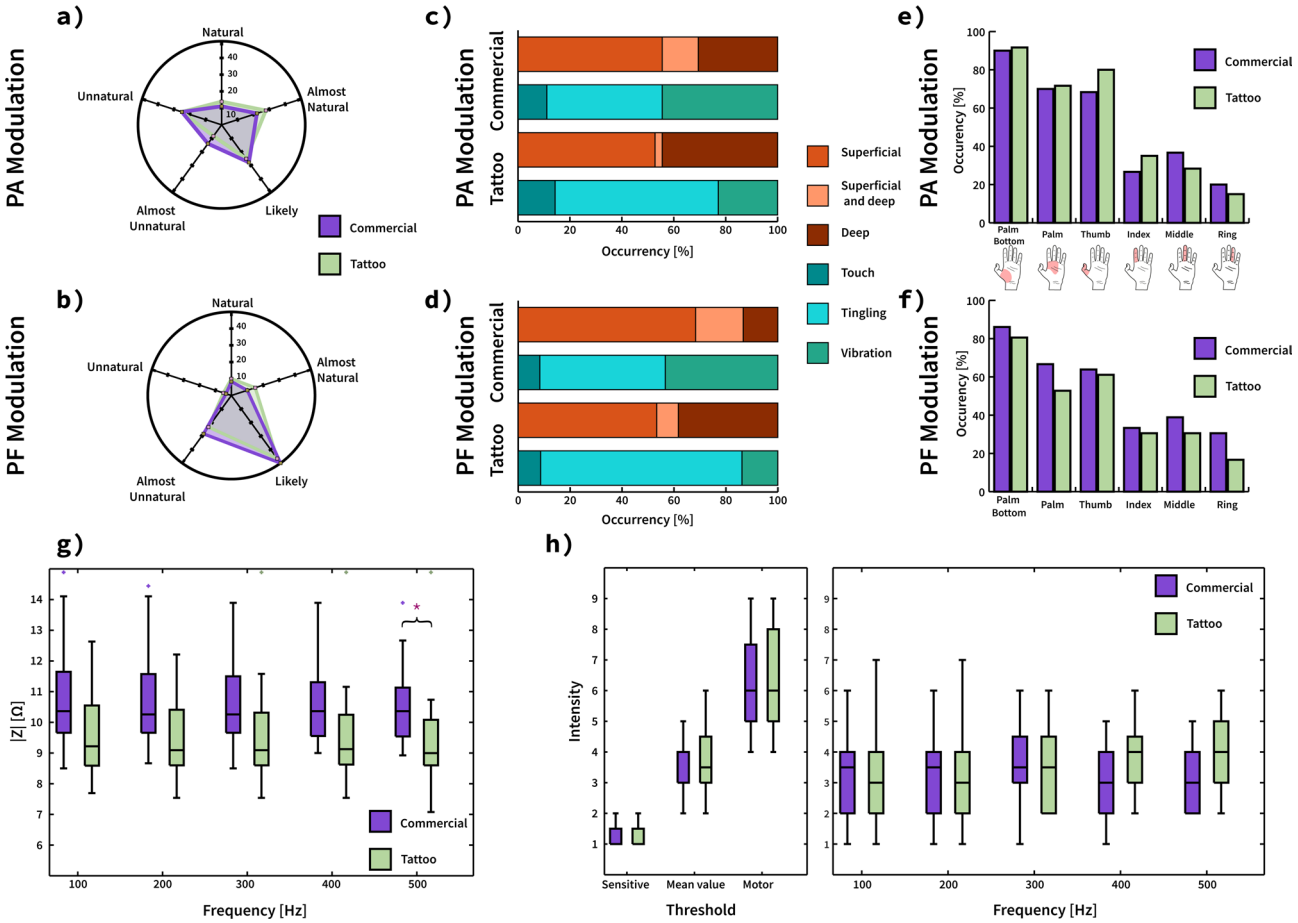

Fig. 3. Somatotopic sensation investigation. The quality of the sensations induced by using the Ag/AgCl electrodes and the tattoo electrodes appears to be comparable both when the amplitude (**a**) and the frequency (**b**) vary, although in this case, the somatosensations reported by using the tattoos described as "almost natural" or "natural" appear to be more significant respect to the ones induced with Ag/AgCl electrodes. The sensations induced are mainly of "vibration" using the wet electrodes, while mainly of "tingling" with the tattoo electrodes. Furthermore, a modification in the depth of the sensation is evident both when the frequency and the amplitude (**c**) of stimulation (**d**) vary. The location of the induced sensations is consistent between the two technologies used. However, the commercial electrodes show a higher coverage of the total area of the hand both when the amplitude (**e**) and the frequency (**f**) vary. At the same time as investigating the sensations induced by changing the frequency, the impedances of the electrodes were recorded (**g**). The intensity of the sensations caused by the two electrodes appears to be consistent. However, when the frequency increases, the sensations induced with the tattoo become more intense than those induced with the commercial ones (**h**).

sensations described as located in "deep" with respect to Ag/AgCl technology (38,33% vs. 13,33%). Tattoo electrodes reported a global coverage of the hand consistent with Ag/AgCl technology. During frequency modulation, the impedance of the electrodes was computed, as shown in Fig. 3g. At the frequencies of use, the impedance of the tattoos appears to be lower than that of the Ag/AgCl electrodes. A statistical difference was observed between the impedances of the electrodes at a frequency of 500 Hz. This effect is attributed to the capacitive nature of dry tattoo electrodes. As the stimulation frequency increases, the capacitance of the electrode-skin interface is bypassed, effectively reducing its contribution to the impedance. Therefore, this reduction in impedance also appears to affect the intensity of the induced sensations, which are generally described as more intense by participants, as shown in Fig. 3f.

Discussion

Ultra comfortable tattoo electrodes for sensory feedback restoration

The proposed method utilizes ultra-thin Parylene C electrodes for non-invasive human medical applications. While temporary tattooable electrodes have been widely used for biomonitoring, this study investigates their potential for sensory feedback restoration. Non-invasive transcutaneous electrical nerve stimulation involves challenges related to both stimulation algorithms and the technological development of stimulating electrodes. Electrodes must maintain stability throughout a full working day, enabling continuous use of the prosthetic system for the entire working day. Therefore, electrode durability and stability are critical for daily operation. The ultra-

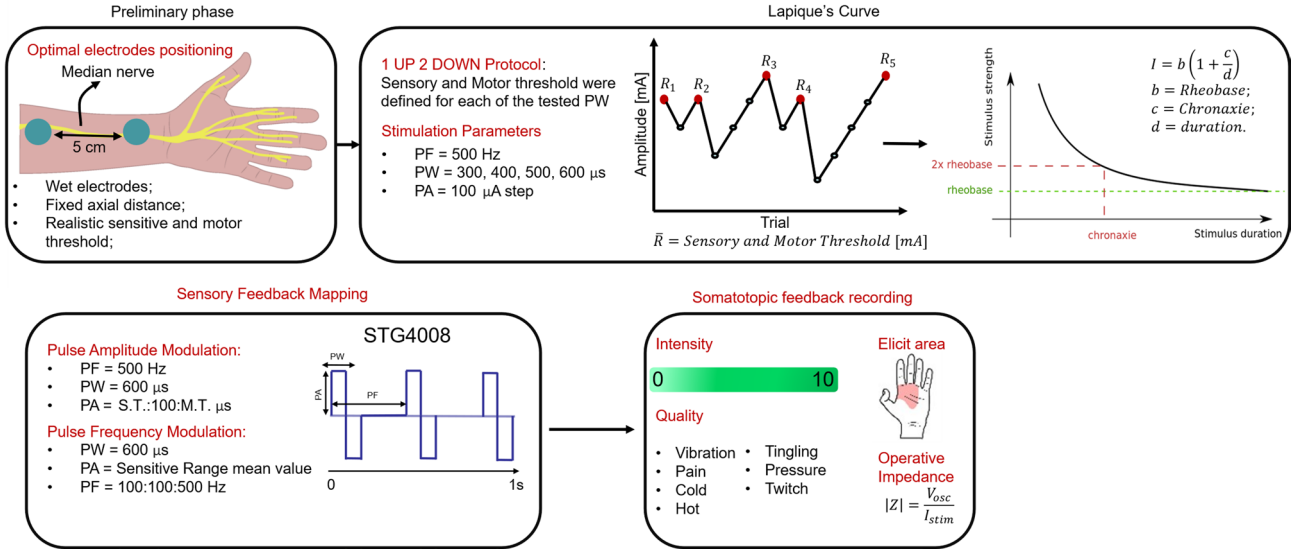

Fig. 4. Ultra-comfortable tattoo electrodes validation protocol.

conformable electrodes demonstrated stable performance over nine hours of use in a controlled environment and consistently induced somatosensory sensations in all twelve healthy participants. This approach addresses the discomfort commonly associated with commercial silver/silver chloride (Ag/AgCl) electrodes, particularly in sensory feedback applications where user comfort is critical. Additionally, the weak electrostatic interaction of the proposed electrodes provides a stable electrode-skin interface, preventing skin irritation throughout the study. These features are essential for daily use and position the ultra-thin tattoo electrodes as strong candidates for restoring sensory feedback.

Strength duration curve

Lapicque curve analysis allows us to objectively assess the operational behavior of tattoo technology, i.e., the ability to stimulate peripheral nerve tissue. To the best of our knowledge, no studies have analyzed the behavior of stimulation electrodes by trying to objectivize electrode performance through physiology. The described approach shows that dry technology is comparable to the gold standard represented by Ag/AgCl electrodes, showing an absence of statistical differences for both rheobase and chronaxie values for sensory and motor pathways. By defining and comparing the size of the sensory area of each subject, it was possible to observe that it is not influenced by the type of electrode used.

Elicitation of somatotopic sensations

Through the modulation of the parameters and the investigation of the sensations induced by the stimulation, it was possible to observe that the tattoo electrodes allow obtaining a behavior comparable to that of the wet electrodes, both from the point of view of the areas of the hand excited and from the point of view of the quality of the sensations declared, which are consistent between the two types of electrodes. However, the behavior of the tattoo electrodes was generally appreciated more by the subjects involved in the test. As with commercial technology, the tattoo electrodes were able to induce sensations along the main regions of the hand where the median nerve is innervated, proving capable of being used in sensory feedback applications where discriminating between different areas of the hand is essential.

Limitations and future directions

Even if promising results have been presented in this paper, the methodologies presented several limitations that should be kept in account. First, the participant group was composed of only 12 healthy subjects, thus limiting the generalizability of the results. A larger cohort, including amputees, should be considered in successive studies, thus improving the robustness of results. Furthermore, each subject participated in the tests only once, and no data was collected that could show the stability of the sensations over time. Second, the stimulation tests were performed in a controlled environment and with subjects in resting conditions. To represent a situation closer to reality, it would be necessary to translate the experiments outside of the laboratory into daily life activities. To do this, the electrodes should be incorporated into a wearable transcutaneous electrical stimulation system with a sufficient voltage compliance and stimulation current to deliver sensory feedback[89–91]. In addition, tests on amputees wearing the entire prosthetic system equipped with the proposed electrodes and a fully wearable sensory feedback system should be performed over a longer period of time, taking into account the variation of perceived sensation due to the prolonged use of electrodes over time. Addressing these limitations will be essential for ensuring that tattoo electrodes can reliably support broader clinical use.

Conclusion

In this paper, we developed ultra-conformable tattoo electrodes for non-invasive electrical stimulation of peripheral nervous tissues using a nanometer-thick Parylene C patch and gold film as the active area. The electrode impedance was analyzed and monitored over nine hours, showing a variation of about 8% at a frequency of 500 Hz. We compared the tattoo technology to the Ag/AgCl technology, commonly used for TENS stimulation, through an innovative analysis based on observing the effects on physiological parameters like rheobase and chronaxie. Although there are no statistical differences between the two technologies, the effective area for somatotopic stimulation is larger with tattoos than with commercial electrodes. We also collected data on the sensations induced by both technologies, demonstrating that the descriptions of these sensations are consistent with those produced by dry or wet electrodes. We have thus shown that tattoo technology can be used in fields such as sensory feedback, where the wearability of the components is a key factor for integrating with prosthetic systems. Given the demonstrated effectiveness of tattoo technology in electrical stimulation, we believe that its mechanical characteristics—high flexibility and ability to follow skin folds and deformations—could be a crucial advantage in sensory stimulation for amputees, allowing electrodes to be placed at non-regular points, such as on the stump.

Methods

Tattoo electrodes fabrications

Tattoo electrodes were fabricated on a 125 µm-thick Poly(Ethylene Naphthalate) (PEN) substrate, which was employed as a carrier for the whole fabrication procedure. Above it, a sacrificial layer of Poly(Vinyl Alcohol) (PVA, 6% in deionized water) was deposited throughout a standard spin coating technique and then baked at 90 °C on a hot plate for 10 min. On top of it, a 500 nm-thick Parylene C layer was deposited via Chemical Vapor Deposition (CVD). Finally, gold electrodes, with a thickness in the range of 50–70 nm, were thermally evaporated using a shadow mask, creating an active electrode area with a diameter of about 2.5 cm.

The tattoo interconnection system was fabricated on a 13 µm-thick polyimide (KAPTON) substrate. A connecting stripe was deposited by inkjet printing gold ink (DryCure Au-J 1010B) onto the substrate, followed by annealing at 120 °C for 2 h.

The thickness characterization of the deposited films was performed through the profilometer Dektak XT by Bruker, Billerica, MA, USA.

The described fabrication process led to the development of circular tattoo electrodes. The shape of the electrodes was defined in agreement with the literature[32,34,36,38,41].

The fabricated electrodes underwent different validation processes aimed at evaluating the electrode/skin impedance, extracting the strength-duration curve, and characterizing the evoked sensations. The experimental protocol was approved by the University of Cagliari ethical committee (N. 0191672), and the research was performed in accordance with the relevant guidelines and regulations in compliance with the Declaration of Helsinki. All the subjects agreed to participate in the study and signed informed consent.

Electrode/Skin contact impedance evaluation

To evaluate the electrode/skin impedance, a healthy participant (a 28-year-old male) was asked to sit in a chair in a comfortable position with his right arm placed on a table. The choice of the right arm rather than the left one was arbitrary because of the human body's symmetry with respect to the sagittal plane. Based on biological landmarks, the medial face of the forearm was located, and thus, a scrub was used to remove the corneous layer. Subsequently, the tattoo electrode was placed at the center of the cleaned area.

The electrode-skin contact impedance analysis was carried out, varying the stimulation frequency in the range of 20–500 Hz, and measuring the impedance using an Agilent 4284 A precision LCR meter (Agilent Technologies Inc., Santa Clara, CA, USA).

Three diameter values (i.e., 10 mm, 20 mm, and 25 mm) were tested for each tattoo electrode to find the optimal dimension. Such values were defined in agreement with the literature since these are the most commonly used electrode sizes[32,36,38,41]. Additionally, 10 specimens were tested for each diameter to minimize inter-participant variability in contact impedance.

Finally, the obtained results were compared to the impedance measured of five commercial pre-gelled electrodes connected in parallel[51,79].

Electrode storage capacitance was investigated through cyclic voltammetry as reported in Ganji et al.[80]. Cyclic Voltammetry was done using Autolab IMP (Metrohm Italiana Srl, Italy) by applying a voltage sweep from − 0.6 V to 0.6 V at a scan rate of 100 mV/s across five repetitions. The resulting curve was used to calculate the charge storage capacity of the Tattoo electrodes using the NOVA software.

The experimental setup is shown in Figure S1 in the Supplementary Materials.

Experimental setup for electrode validation.

Twelve healthy subjects (4 females and 8 males) with an average age of 26.75 ± 2.45 years were enrolled in the trials to extract the strength-duration curve and characterize the sensations elicited with the two types of electrodes.

Each participant was asked to sit in a chair in a comfortable position with their left arm placed on a table. The median nerve path along the forearm was located based on biological landmarks. In this phase, no scrub or skin preparation procedure was performed. The choice of stimulating the median nerve was attributed to anatomical considerations since it innervates the thumb's thenar eminence, the palmar side, the index, middle, and half of the ring finger[89].

Subsequently, a pair of both tattoo and commercial, circular (25 mm diameter) and auto-adhesive electrodes (TensCare Ltd, Epsom, UK) was placed in the region of interest, with a distance of 50 mm between the active and

counter electrodes. Such commercial wet electrodes were chosen since they were developed for electrostimulation and are widely used in the literature[38–41,92]. Both pairs of electrodes were connected to the electric stimulator STG4008 (Multichannel System MCS GmbH, Reutlingen, DE) for stimulus delivery.

In agreement with the literature, a symmetric biphasic square wave was used since it induces charge transfer according to the phase-preventing galvanic process that could cause tissue damage[90,93]. The stimulation parameters considered were the Pulse Amplitude (PA), the Pulse Width (PW), and the Pulse Frequency (PF).

The delivered stimuli were monitored by an oscilloscope (Teledyne T3DSO1202A, 200 MHz, CA, USA), connected to the electrical stimulator by insulated probes, while the adopted stimulation parameters were recorded using a custom-made Graphical User Interface (GUI) developed in C# using Visual Studio 2019 (Microsoft, Redmond, WA, USA). The same GUI was used to allow participants to characterize the referred elicited sensations in terms of location, naturalness (i.e., a five-point scale ranging from unnatural to natural), depth (i.e., superficial, superficial and deep, deep), intensity (i.e., a scale from 0 to 10), and quality. Quality descriptors were derived from the literature[38,39,41,89].

The experimental setup is shown in Fig. S3 in the Supplementary Materials.

Experimental protocol for electrode validation

The experimentation was carried out in time slots of 2 h with resting phases to avoid habituation.

To extract the strength-duration curve, the following steps were applied:

The minimum current amplitude to elicit a sensation (sensory threshold) and the maximum one that elicits a sensation without producing a muscular contraction were determined. Thresholds were obtained using a 1-up / 2-down adaptive psychophysics method[94,95] with 100 μA steps and a threshold set at five reversals. The threshold was obtained for four different stimulation durations (300 μs, 400 μs, 500 μs, and 600 μs). This test was performed for stimulation with a train of pulses of 1s at 500 Hz. Two modulations were adopted to characterize the sensations. In the amplitude modulation, the PW, the PF, and the stimulus length were kept constant at 600 μs, 500 Hz, and 1 s, respectively, while the PA varied between three values (sensory threshold, motor threshold, and mean sensitive range value). In the frequency modulation, the PW and the stimulus length were maintained constant at 600 μs and 1 s, respectively, while the PF varied between 100 Hz and 500 Hz in steps of 100 Hz. The amplitude was fixed to the mean value between the sensory and motor threshold, to be sure of being capable of eliciting a sensory sensation.

For each stimulus, the electrode/skin impedance value was evaluated with the oscilloscope, and the participants described the perceived sensations using the GUI.

The experimental protocol was carried out for each pair of electrodes (i.e., tattoo and commercial) in a random order to avoid measurement bias.

Data analysis

All data were exported and processed offline in MATLAB (R2020a, MathWorks, Natick, MA, USA).

Data obtained from the detection threshold was used to fit Lapicque's Eqs. [90,91], extracting the value of rheobase current and chronaxie time[37,82,85] :

$$I = b(1 + \frac{c}{d})$$

Where b is the rheobase current, c is the chronaxie, and d is the pulse width of stimulation. Lapicque's equation was fitted using a robust linear least-squares fitting method based on the bisquare weights method. Somatosensation stimulation area (A_{som}) was computed as:

$$A_{som} = A_M - A_s$$

where A_M and A_s are the areas below Lapicque's equation for motor and sensory threshold, respectively. The area below the curves was computed as:

$$A = \int_{300\mu\ s}^{600\mu\ s} b\left(1 + \frac{c}{x}\right) dx$$

The ratio between the somatosensory area relative to electrical stimulation with tattoo and Ag/AgCl electrodes ($A_{somTatt}$ and $A_{somComm}$, respectively) was computed as:

$$Ratio = \frac{A_{somTatt}}{A_{somComm}}$$

The quality and location of induced sensations were collected for each subject through a custom GUI. The data derived from each subject were analyzed together in order to have a global view of the effect of stimulation as reported in Paolini et al.[92] and in Collu et al.[37]. Location and quality of sensations were analyzed in terms of occurrences, i.e., as the number of times a sensation was reported in a specific location or with a certain quality, with respect to the total number of reported sensations.

Statistical analysis

To compare the performance of tattoo and commercial electrodes, a statistical analysis was carried out. The Shapiro-Wilk test was adopted for evaluating the normality of data distribution, and it was non-Gaussian. Therefore, a null hypothesis test using the Wilcoxon signed-rank test is conducted, considering an alpha

significance level $\alpha = 0.05$. Moreover, a Wilcoxon signed-rank test was also used to verify whether the ratio between the somatosensation area for tattoo and commercial electrodes was different from 1.

Data availability

All technical details for producing the figures are enclosed in the manuscript. The simulated and measured data presented in this paper can be found at Open Science Framework (Ultra-conformable Tattoo electrodes for providing sensory feedback via transcutaneous electrical nerve stimulation, 2025).

Received: 23 May 2025; Accepted: 22 September 2025
Published online: 27 October 2025

References

1. Raspopovic, S. et al. Restoring natural sensory feedback in Real-Time bidirectional hand prostheses. *Sci. Transl Med.* **6**, 222ra19 (2014).
2. George, J. A. et al. Biomimetic sensory feedback through peripheral nerve stimulation improves dexterous use of a bionic hand. *Sci. Robot*. **4**, eaax2352 (2019).
3. Schiefer, M., Tan, D., Sidek, S. M. & Tyler, D. J. Sensory feedback by peripheral nerve stimulation improves task performance in individuals with upper limb loss using a myoelectric prosthesis. *J Neural Eng.* **13**, 016001 (2015).
4. Pasluosta, C., Kiele, P. & Stieglitz, T. Paradigms for restoration of somatosensory feedback via stimulation of the peripheral nervous system. *Clin. Neurophysiol.* **129**, 851–862. https://doi.org/10.1016/j.clinph.2017.12.027 (2018).
5. Dhillon, G. S. & Horch, K. W. Direct neural sensory feedback and control of a prosthetic arm. *IEEE Trans. Neural Syst. Rehabil. Eng.* **13**, 468–472 (2005).
6. Valle, G. et al. Biomimetic intraneural sensory feedback enhances sensation Naturalness, tactile Sensitivity, and manual dexterity in a bidirectional prosthesis. *Neuron* **100**, 37–45e7 (2018).
7. Rognini, G. et al. Multisensory bionic limb to achieve prosthesis embodiment and reduce distorted phantom limb perceptions. *J. Neurol, Neurosurg. Psychiatry.* **90**, 833–836. https://doi.org/10.1136/jnnp-2018-318570 (2019).
8. Mulvey, M. R., Fawkner, H. J., Radford, H. E. & Johnson, M. I. Perceptual embodiment of prosthetic limbs by transcutaneous electrical nerve stimulation. *Neuromodulation* **15**, 42–47 (2012).
9. Biddiss, E., Beaton, D. & Chau, T. Consumer design priorities for upper limb prosthetics. *Disabil. Rehabil Assist. Technol.* **2**, 346–357 (2007).
10. Biddiss, E. & Chau, T. Upper-limb prosthetics: critical factors in device abandonment. *Am. J. Phys. Med. Rehabil.* **86**, 977–987 (2007).
11. Osborn, L. E. et al. Sensory stimulation enhances phantom limb perception and movement decoding. *J. Neural Eng.* **17**, 056006 (2020).
12. Dietrich, C. et al. Leg prosthesis with somatosensory feedback reduces phantom limb pain and increases functionality. *Front Neurol.* **9**, 270 (2018).
13. Antfolk, C. et al. Artificial Redirection of sensation from prosthetic fingers to the Phantom hand map on transradial amputees: vibrotactile versus mechanotactile sensory feedback. *IEEE Trans. Neural Syst. Rehabil. Eng.* **21**, 112–120 (2013).
14. Thomas, N., Ung, G., Ayaz, H. & Brown, J. D. Neurophysiological evaluation of haptic feedback for myoelectric prostheses. *IEEE Trans. Hum. Mach. Syst.* **51**, 253–264 (2021).
15. Saal, H. P. & Bensmaia, S. J. Biomimetic approaches to bionic touch through a peripheral nerve interface. *Neuropsychologia* **79**, 344–353 (2015).
16. Raspopovic, S., Valle, G. & Petrini, F. M. Sensory feedback for limb prostheses in amputees. *Nat. Mater.* **20**, 925–939 (2021).
17. Bensmaia, S. J., Tyler, D. J. & Micera, S. Restoration of sensory information via bionic hands. *Nat. Biomed. Eng.* https://doi.org/10.1038/s41551-020-00630-8 (2020).
18. Charkhkar, H. et al. High-density peripheral nerve cuffs restore natural sensation to individuals with lower-limb amputations. *J Neural Eng* **15**, (2018).
19. Naples, G. G., Mortimer, J. T., Scheiner, A. & Sweeney, J. D. *A spiral nerve cuff electrode for peripheral nerve stimulation*. *IEEE Trans. BIOMEDICAL ENGINEERING* **35** (1988).
20. Tyler, D. J. Neural interfaces for somatosensory feedback: Bringing life to a prosthesis. *Curr. Opin. Neurol.* **28**, 574–581. https://doi.org/10.1097/WCO.0000000000000266 (2015).
21. Petrini, F. M. et al. Six-Month assessment of a hand prosthesis with intraneural tactile feedback. *Ann. Neurol.* **85**, 137–154 (2019).
22. Boretius, T. et al. A transverse intrafascicular multichannel electrode (TIME) to interface with the peripheral nerve. *Biosens. Bioelectron.* **26**, 62–69 (2010).
23. Čvančara, P. et al. Bringing sensation to prosthetic hands—chronic assessment of implanted thin-film electrodes in humans. *Npj Flex. Electronics* **7**, (2023).
24. George, J. A. et al. Long-term performance of Utah slanted electrode arrays and intramuscular electromyographic leads implanted chronically in human arm nerves and muscles. *J Neural. Eng.* **17**, (2020).
25. Navarro, X. et al. A critical review of interfaces with the peripheral nervous system for the control of neuroprostheses and hybrid bionic systems. *J. Peripher. Nerv. Syst.* **10**, 229–258. https://doi.org/10.1111/j.1085-9489.2005.10303.x (2005).
26. Tan, D. W. et al. A neural interface provides long-term stable natural touch perception. *Sci. Transl Med.* **6**, 257ra138–257ra138 (2014).
27. Ortiz-Catalan, M., Brånemark, R., Håkansson, B. & Delbeke, J. *On the viability of implantable electrodes for the natural control of artificial limbs: review and discussion*. *BioMedical Eng. OnLine* **11** (2012). http://www.biomedical-engineering-online.com/content/11/33REVIEW
28. Page, D. M. et al. Discriminability of multiple cutaneous and proprioceptive hand percepts evoked by intraneural stimulation with Utah slanted electrode arrays in human amputees. *J Neuroeng. Rehabil* **18**, (2021).
29. Wendelken, S. et al. Restoration of motor control and proprioceptive and cutaneous sensation in humans with prior upper-limb amputation via multiple Utah slanted electrode arrays (USEAs) implanted in residual peripheral arm nerves. *J Neuroeng. Rehabil* **14**, (2017).
30. Forst, J. C. et al. Surface electrical stimulation to evoke referred sensation. *J. Rehabil Res. Dev.* **52**, 397–406 (2015).
31. Johnson, M. I. Transcutaneous electrical nerve stimulation (TENS). in Encyclopedia of Life Sciences (Wiley, doi:https://doi.org/10.1002/9780470015902.a0024044. (2012).
32. D'Anna, E. et al. A somatotopic bidirectional hand prosthesis with transcutaneous electrical nerve stimulation based sensory feedback. *Sci Rep* **7**, (2017).
33. Ding, K. et al. Towards machine to brain interfaces: sensory stimulation enhances sensorimotor dynamic functional connectivity in upper limb amputees. *J Neural Eng* **17**, (2020).
34. Pan, L. et al. Evoking haptic sensations in the foot through high-density transcutaneous electrical nerve stimulations. *J Neural Eng* **17**, (2020).

35. Chai, G., Sui, X., Li, S., He, L. & Lan, N. Characterization of evoked tactile sensation in forearm amputees with transcutaneous electrical nerve stimulation. *J Neural Eng* **12**, (2015).
36. Osborn, L. E. et al. Prosthesis with neuromorphic multilayered e-dermis perceives touch and pain. *Sci. Robot.* **3**, eaat3818 (2018).
37. Collu, R., Earley, E. J., Barbaro, M. & Ortiz-Catalan, M. Non-rectangular neurostimulation waveforms elicit varied sensation quality and perceptive fields on the hand. *Sci. Rep.* **13**, 1588 (2023).
38. Scarpelli, A., Demofonti, A., Terracina, F., Ciancio, A. L. & Zollo, L. Evoking apparent moving sensation in the hand via transcutaneous electrical nerve stimulation. *Front Neurosci* **14**, (2020).
39. Demofonti, A., Scarpelli, A., Cordella, F. & Zollo, L. Modulation of sensation intensity in the lower limb via Transcutaneous Electrical Nerve Stimulation. in *Proceedings of the Annual International Conference of the IEEE Engineering in Medicine and Biology Society, EMBS* 6470–6474Institute of Electrical and Electronics Engineers Inc., (2021). https://doi.org/10.1109/EMBC46164.2021.9630871
40. Demofonti, A. et al. Somatotopical feedback restoration in the lower limb through TENS: a feasibility study. in *2021 VII Congress of the National Group of Bioengineering (GNB)* (2020).
41. Scarpelli, A. et al. Eliciting force and slippage in upper limb amputees through transcutaneous electrical nerve stimulation (TENS). *IEEE Trans. Neural Syst. Rehabil. Eng.* **32**, 3006–3017 (2024).
42. Scarpelli, A., Cordella, F. & Zollo, L. Encoding algorithms for somatotopic restoration of somatic sensations in the upper-limb: a systematic review. *J. Neural Eng.* https://doi.org/10.1088/1741-2552/ade503 (2025).
43. Yoo, J., Yan, L., Lee, S., Kim, H. & Yoo, H. J. A wearable ECG acquisition system with compact planar-fashionable circuit board-based shirt. *IEEE Trans. Inf Technol. Biomed.* **13**, 897–902 (2009).
44. Hong, S. & Coté, G. Minimization of parasitic capacitance between skin and Ag/AgCl dry electrodes. *Micromachines (Basel)* **15**, (2024).
45. Preatoni, G., Dell'Eva, F., Valle, G., Pedrocchi, A. & Raspopovic, S. Reshaping the full body illusion through visuoelectro-tactile sensations. *PLoS One* **18**, (2023).
46. Chee, L. et al. Optimally-calibrated non-invasive feedback improves amputees' metabolic consumption, balance and walking confidence. *J Neural Eng* **19**, (2022).
47. Liang, W. et al. Study of tactile sensation somatotopy and homology between projected fingers in residual limb and natural fingers in intact limb. *IEEE Trans. Neural Syst. Rehabil. Eng.* **31**, 636–645 (2023).
48. Zhang, J. et al. Evaluation of multiple perceptual qualities of transcutaneous electrical nerve stimulation for evoked tactile sensation in forearm amputees. *J Neural Eng* **19**, (2022).
49. Pena, A. E., Abbas, J. J. & Jung, R. Channel-hopping during surface electrical neurostimulation elicits selective, comfortable, distally referred sensations. *J Neural Eng* **18**, (2021).
50. Wang, Y. et al. All-weather, natural silent speech recognition via machine-learning-assisted tattoo-like electronics. *Npj Flex. Electronics* **5**, (2021).
51. Spanu, A. et al. Parylene C-Based, breathable tattoo electrodes for High-Quality Bio-Potential measurements. *Front Bioeng. Biotechnol* **10**, (2022).
52. Steenbergen, N. et al. Surface electromyography using dry polymeric electrodes. *APL Bioeng* **7**, (2023).
53. Ferri, J. et al. A new method for manufacturing dry electrodes on textiles. Validation for wearable ECG monitoring. *Electrochem Commun* **136**, (2022).
54. Elango, P. F. M. et al. Dry electrode geometry optimization for wearable ECG devices. *Appl Phys. Rev* **10**, (2023).
55. Yang, L. et al. Insight into the contact impedance between the electrode and the skin surface for electrophysical recordings. *ACS Omega*. **7**, 13906–13912 (2022).
56. Li, G., Wang, S. & Duan, Y. Y. Towards conductive-gel-free electrodes: Understanding the wet electrode, semi-dry electrode and dry electrode-skin interface impedance using electrochemical impedance spectroscopy fitting. *Sens. Actuators B Chem.* **277**, 250–260 (2018).
57. Habibzadeh Tonekabony Shad, E., Molinas, M. & Ytterdal, T. Impedance and noise of passive and active dry EEG electrodes: A review. *IEEE Sens. J.* **20**, 14565–14577 (2020).
58. Mascia, A. et al. Impedance characterization and modeling of Gold, Silver, and PEDOT:PSS Ultra-Thin tattoo electrodes for wearable bioelectronics. *Sensors* **25**, 4568 (2025).
59. Zhao, Y. et al. Ultra-conformal skin electrodes with synergistically enhanced conductivity for long-time and low-motion artifact epidermal electrophysiology. *Nat Commun* **12**, (2021).
60. Shin, J. H., Choi, J. Y., June, K., Choi, H. & Kim, T. il. Polymeric conductive Adhesive-Based ultrathin epidermal electrodes for Long-Term monitoring of electrophysiological signals. *Advanced Materials* **36**, (2024).
61. Kim, D. H. *et al. Epidermal Electronics*. https://www.science.org
62. Kateb, P. et al. Printable, adhesive, and self-healing dry epidermal electrodes based on PEDOT:PSS and polyurethane diol. *Flexible Print. Electronics* **8**, (2023).
63. Yang, S. et al. Highly adhesive and stretchable epidermal electrode for bimodal recording patch. *ACS Appl. Mater. Interfaces*. **16**, 43880–43891 (2024).
64. Mascia, A. et al. Wearable system based on Ultra-Thin parylene C tattoo electrodes for EEG recording. *Sensors* **23**, (2023).
65. Spanu, A. et al. Epidermal electrodes with Ferrimagnetic/Conductive properties for biopotential recordings. (2022). https://doi.org/10.3390/bioengineering
66. Valeriani, D., Kalckert, A., Eagleman, D. M. & Perrotta, M. V. *The Future of Sensory Substitution, Addition, and Expansion via Haptic Devices*.
67. Svensson, P., Wijk, U., Björkman, A. & Antfolk, C. A review of invasive and non-invasive sensory feedback in upper limb prostheses. *Expert Review of Medical Devices* vol. 14 439–447 Preprint at (2017). https://doi.org/10.1080/17434440.2017.1332989
68. Shi, Y. et al. Self-powered electro-tactile system for virtual tactile experiences. *Sci Adv* **7**, (2021).
69. Yao, K. et al. Encoding of tactile information in hand via skin-integrated wireless haptic interface. *Nat. Mach. Intell.* **4**, 893–903 (2022).
70. Lin, W. et al. *Super-Resolution wearable electrotactile rendering system*. *Sci Adv* **8** (2022). https://www.science.org
71. Xu, B. et al. An epidermal stimulation and sensing platform for sensorimotor prosthetic Control, management of lower back Exertion, and electrical muscle activation. *Adv. Mater.* **28**, 4462–4471 (2016).
72. Ying, M. et al. Silicon nanomembranes for fingertip electronics. *Nanotechnology* **23**, (2012).
73. Abbass, Y., Saleh, M., Dosen, S. & Valle, M. Embedded electrotactile feedback system for hand prostheses using matrix electrode and electronic skin. *IEEE Trans. Biomed. Circuits Syst.* **15**, 912–925 (2021).
74. Nawrocki, R. A. et al. Self-Adhesive and Ultra-Conformable, Sub-300 Nm dry Thin-Film electrodes for surface monitoring of biopotentials. *Adv Funct. Mater* **28**, (2018).
75. Nawrocki, R. A. Super- and Ultrathin Organic Field-Effect Transistors: from Flexibility to Super- and Ultraflexibility. *Advanced Functional Materials* vol. 29 Preprint at (2019). https://doi.org/10.1002/adfm.201906908
76. Wang, Y. et al. Electrically compensated, tattoo-like electrodes for epidermal electrophysiology at scale. *Sci Adv* **6**, (2020).
77. Wang, S. et al. Mechanics of epidermal electronics. *Journal Appl. Mech. Trans. ASME* **79**, (2012).
78. Ganji, M., Tanaka, A., Gilja, V., Halgren, E. & Dayeh, S. A. Scaling effects on the electrochemical stimulation performance of Au, Pt, and PEDOT:PSS electrocorticography arrays. *Adv Funct. Mater* **27**, (2017).
79. Pani, D. et al. Fully Textile, PEDOT:PSS based electrodes for wearable ECG monitoring systems. *IEEE Trans. Biomed. Eng.* **63**, 540–549 (2016).

80. Boinagrov, D., Loudin, J. & Palanker, D. Strength-duration relationship for extracellular neural stimulation: numerical and analytical models. *J. Neurophysiol.* **104**, 2236–2248 (2010).
81. Wessale, J. L., Geddes, L. A., Grego~', Ayers, M. & Foster, K. S. *Comparison of rectangular and exponential current pulses for evoking sensation*. *Annals Biomedical Engineering* **20** (1992).
82. Sahin, M. & Tie, Y. Non-rectangular waveforms for neural stimulation with practical electrodes. *J. Neural Eng.* **4**, 227–233 (2007).
83. Foutz, T. J. & McIntyre, C. C. Evaluation of novel stimulus waveforms for deep brain stimulation. *J Neural Eng* **7**, (2010).
84. Wongsarnpigoon, A. & Grill, W. M. Energy-efficient waveform shapes for neural stimulation revealed with a genetic algorithm. *J Neural Eng* **7**, (2010).
85. Thomas, N., Osborn, L., Moran, C., Fifer, M. & Christie, B. Wrist Posture Unpredictably Affects the Perception of Transcutaneous Electrical Nerve Stimulation. Preprint at (2023). https://doi.org/10.1101/2023.11.07.23298213
86. Earley, E. J. & Ortiz-Catalan, M. Neurostimulation Perception Obeys Strength-Duration Curves and is Primarily Driven by Pulse Amplitude. in *International IEEE/EMBS Conference on Neural Engineering, NER* 2023-AprilIEEE Computer Society, (2023).
87. Lapicque, L. & Definition Experimentale, L. *Comptes Rendus De l'Académie Des. Sci.* **67**, 280–283 (1909).
88. Geddes, L. A. & Bourland, J. D. The Strength-Duration curve. *IEEE Trans. Biomed. Eng.* **BME-32**, 458–459 (1985).
89. Paolini, R. et al. A novel portable device and validation procedure for transcutaneous electrical nerve stimulation. *Wearable Technol.* **6**, e40 (2025).
90. Collu, R. et al. Wearable high voltage compliant current stimulator for restoring sensory Feedback. *Micromachines (Basel)* **14**, 782 (2023).
91. Collu, R. et al. Development of an electrical current stimulator for controlling biohybrid machines. *Sci. Rep.* **15**, 22473 (2025).
92. Demofonti, A. et al. Restoring somatotopic sensory feedback in lower limb amputees through noninvasive nerve stimulation. *Cyborg Bionic Syst.* **6**, 0243 (2025).
93. Mereu, F. et al. A sensory feedback neural stimulator prototype for both implantable and wearable applications. *Micromachines (Basel)* **15**, 480 (2024).
94. Kaernbach, C. Simple adaptive testing with the weighted up-down method. *Percept. Psychophys.* **49**, 227–229 (1991).
95. García-Pérez, M. A. Forced-choice staircases with fixed step sizes: asymptotic and small-sample properties. *Vision Res.* **38**, 1861–1881 (1998).

Acknowledgements

The authors thank the subjects who participated in the study for their time and effort.

Author contributions

R.C., A.M., R.P., F.C., and A.D. designed the study. R.P., A.M., and R.C. executed the experiments. A.M. fabricated the electrodes. R.C. and R.P. supported data and statistical analysis. R.C. and A.M. prepared the figures. F.C., A.D., L.Z., M.B., and P.C. supervised and coordinated the research. R.C., A.M., and R.P. drafted the manuscript. All the authors reviewed and approved the submitted manuscript.

Funding

This research activity was partially founded from Sardegna Ricerche under the PoC grant with SMARTPATCH (CUP: F23C24001290002) and partially from the National Institute for Insurance against Accidents at Work (INAIL) Prosthetic Center with BioInterNect (CUP: E57G23000280005).

Declarations

Competing interests

The authors declare no competing interests.

Additional information

Supplementary Information The online version contains supplementary material available at https://doi.org/10.1038/s41598-025-21599-x.

Correspondence and requests for materials should be addressed to C.R., Z.L., B.M. or C.P.